Molecular Crystals and Liquid Crystals

Publication details, including instructions for authors and subscription information:
http://www.tandfonline.com/loi/gmcl20

A Comparison Between Zeolites and Crystalline State as Reaction Media: Asymmetric Induction During Photocyclization of α-Mesitylacetophenones to 2-Indanols

Arunkumar Natarajan [a] , V. Ramamurthy [a] & Joel T. Mague [b]

[a] Department of Chemistry, University of Miami, Coral Cables, Florida

[b] Department of Chemistry, Tulane University, New Orleans, Louisiana

Version of record first published: 21 Dec 2006

To cite this article: Arunkumar Natarajan, V. Ramamurthy & Joel T. Mague (2006): A Comparison Between Zeolites and Crystalline State as Reaction Media: Asymmetric Induction During Photocyclization of α-Mesitylacetophenones to 2-Indanols, Molecular Crystals and Liquid Crystals, 456:1, 71-84

To link to this article: http://dx.doi.org/10.1080/15421400600786355

Mol. Cryst. Liq. Cryst., Vol. 456, pp. 71–84, 2006

ISSN: 1542-1406 print/1563-5287 online
DOI: 10.1080/15421400600786355

Taylor & Francis
Taylor & Francis Group

A Comparison Between Zeolites and Crystalline State as Reaction Media: Asymmetric Induction During Photocyclization of α-Mesitylacetophenones to 2-Indanols

Arunkumar Natarajan
V. Ramamurthy
Department of Chemistry, University of Miami, Coral Cables, Florida

Joel T. Mague
Department of Chemistry, Tulane University, New Orleans, Louisiana

The effectiveness of chiral auxiliaries in inducing diastereoselectivity during photocyclization of ten differnt α-mesitylacetophenones to 2-indanols in crystalline state and as zeolite inclusion complexes has been examined. In the systems examined the chiral auxiliary functioned better within zeolites than in crystals. Crystal structure analysis of three α-mesitylacetophenones revealed that the low chiral induction in the crystalline state is either due to the presence of conformational isomerism in the reactant part of the molecule or the absence of communication between the chiral auxiliary and the reactant part of the ketone.

Keywords: crystalline state; chiral induction; photocyclization; mesitylacetophenones; diastereoselectivity; zeolites; δ-hydrogen abstraction

INTRODUCTION

Achieving high asymmetric induction during photochemical reactions has remained a of great interest over the last few decades [1]. Several thoughtful methodologies are employed both in solid and solution media in order to obtain impressive chiral induction during photochemical

V. R. thanks the NSF (CHE-0212042) for financial support and JTM thanks the Louisiana Board of regents through the Louisiana Educational Quality Support Fund [Grant No. LEQSF (2003-2003)-ENH-TR-67] for the purchase of the Bruker APEX diffractometer.

Address correspondence to Arunkumar Natarajan, Department of Chemistry and Biochemistry, 607 Charles E. Young Drive East, University of California, Los Angeles, CA 90024, USA. E-mail: anatara@chem.ucla.edu; murthy1@miami.edu

reactions [2]. Generally, the crystalline state has been more productive in terms of achieving quantitative stereoselectivity during photochemical reactions. Solid state photoreaction of chiral crystals obtained from achiral molecules, chiral crystals generated *via* ionic chiral auxiliary and covalent chiral auxiliary strategies, and crystals of guest included chiral organic hosts have been successfully used to obtain near quantitative asymmetric induction [3]. Recently we reported the use of covalent chiral auxiliary strategy as an effective approach to achieve high asymmetric induction in various Yang photocyclization reactions in the crystalline state [4]. As an alternative, in this report we show that photoreaction of α-mesitylacetophenone derivatives carrying a covalent chiral auxiliary tend to give high asymmetric induction within faujasite zeolite compared to the crystalline state.

RESULTS AND DISCUSSION

In the past, we have demonstrated that the cavities and the cations present in the faujasite zeolites can be exploited to induce stereoselectivity during photochemical reactions with the help of chiral inductor and chiral auxiliary strategies [5]. Using a variety of reactions such as electocyclizations, geometric isomerizations, oxa-di-π-methane rearrangement reactions, Yang photocyclizations, photoreduction of phenylketones etc., we were able to show that moderate to high stereoselectivity (40–90% enantio/diastereomeric excess) can be obtained within zeolites [6]. The reaction under investigation in this paper is the photomediated δ-hydrogen abstraction reaction of α-mesitylacetophenone (**1a**) leading to 2-phenyl-2-hydroxy-4,6-dimethylindan (**2a**) (Scheme 1) [7]. On photoexcitation, a new stereogenic center is formed in the photoproduct starting from an achiral substrate. The mechanism of this reaction involves a triplet state δ-hydrogen atom abstraction reaction that generates 1,5-biradical. Irradiation of an achiral substrate in solution yields only racemic mixtures of indan photo product. This prompted us to investigate asymmetric induction on this photo product within zeolites and in the crystalline state using the chiral auxiliary strategy.

Photoreaction of compounds **1a–j** in solution, and within faujasite Y zeolite [8] gave exclusively the indan photoproducts (Scheme 1). The chiral mesityl derivatives were synthesized by linking optically pure chiral auxiliaries such as amines and aminoacids at the *para* or the *meta* position of the benzoyl moiety of α-mesitylacetophenone carboxylic acid as an amide linkage (Scheme 1). The photoreaction of the chiral auxiliary linked substrates (**1a–j**) in CH_3CN gave <10% de in photoproducts while the photoreaction within alkali cation exchanged

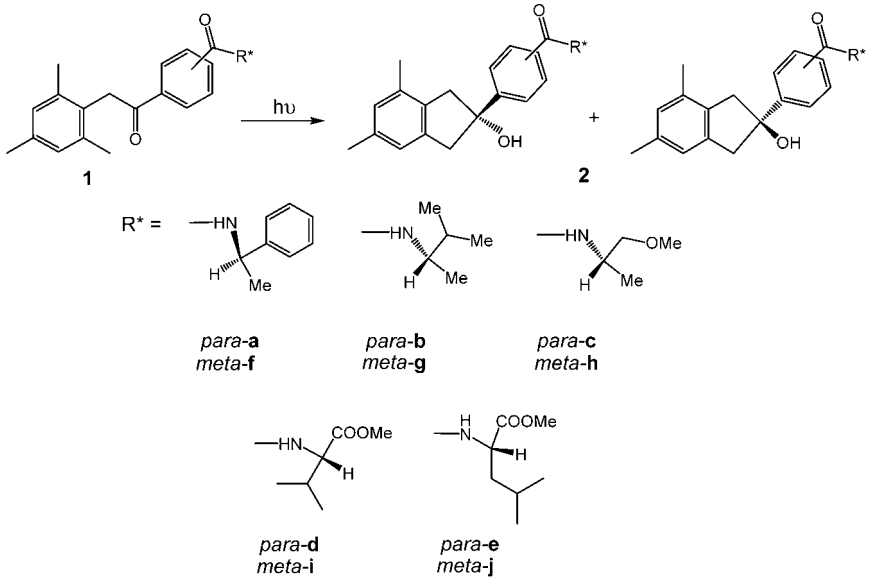

SCHEME 1 Photoreaction of chiral auxiliary linked substrates **1a–j** within zeolites.

zeolites gave significantly high diastereoselectivity. The % de obtained within LiY–CsY exchanged zeolites for *para* and *meta* substituted substrates are presented in Table 1. Maximum of 60% de was obtained on

TABLE 1 % De on Indan Photoproducts (**2a–2j**) Obtained by Photoreaction of *Para*- and *Meta*-Derivatives of α-Mesitylacetophenone in Solution, Crystalline State[a] and Within Zeolites

Substrate	CH_3CN	LiY	NaY	KY	RbY	CsY
1a	1A	47B	60B	42B	10B	6A
1b	0	4A	28A	22B	12B	5B
1c	6A	35A	28A	25A	10A	5A
1d	4A	15A	11A	58A	62A	33A
1e	2A	8A	7A	15A	45A	54A
1f	7A	25A	32A	45B	20B	–
1g	1A	5A	26A	43B	54B	48B
1h	1A	41A	30B	8B	7B	0
1i	2A	5B	74B	60A	23A	6A
1j	4B	32A	57B	23B	5B	–

[a]The % de's obtained during crystalline state photoreaction of substrates **1a–c** are 9, 5 and 22 on the photo products **2a–c** respectively at 14–17% conversions and solid state photoreaction of **1f** gave 48% de on **2f** at 50% conversion.

indan photoproduct (**2a**) within NaY zeolite during photoreaction of *para*-phenylethylamide substituted α-mesitylacetophenone (**1a**). Also the % de's varied depending upon the type of cation present within the zeolite. For example, the % de's obtained on photo product **2a** in alkali metal exchanged MY zeolite are LiY-47, NaY-60, KY-42, RbY-10, CsY-6. The other two amide chiral auxiliaries, 3-methyl-2-butylamide and methoxypropylamide (**1b** and **1c**) gave maximum of 28% and 35% de in NaY and LiY respectively. The above results show that aryl amide (**1a**) is more effective in obtaining enhanced diastereoselectivity than alkyl amide chiral auxiliaries [9]. In anticipation that asymmetric influence can be enhanced when the chiral auxiliary is brought closer to the reaction center, the chiral auxiliaries were coupled to the *meta* position (Table 1). However, the phenyl ethyl amide chiral auxiliary coupled mesitylacetopheone derivative (**1f**) gave only 32% de in the case of NaY, as compared to the corresponding *para* substituted counter part (**3a**) which gave 60% de on the indan photoproduct. Photoreaction of **1f** in KY zeolite gave a slight enhancement (up to 45%) on de of the photo product. Among the *para* substituted amino acid derivatives (**1d** and **1e**), both L-valine methyl ester amide **1d** and L-leusine methyl ester amide **1e** gave enhanced % de on their corresponding indan photo products: 62% and 54% in RbY and CsY, respectively.

On comparing the % de obtained on *meta* substituted alkyl chiral auxiliaries, R(-)-3-methyl-2-butyl amide (**1g**), S(-)methoxy propylamide (**1h**), L-valine methyl ester amide (**1i**) and L-leucine methyl ester amide (**1j**) with their corresponding *para* (**1b–e**) derivatives, it is evident that the *meta* substituted chiral auxiliaries gave better de's as compared to those of the *para* substituted ones. However, in some cases the maximum enhancement of % de was not obtained with the same cation exchanged zeolite when the same chiral auxiliary was linked to *para* and *meta* positions. For instance *para* substituted 3-methyl-2-butylamide chiral auxiliary gave maximum % de of 28% on photoproduct **1b** within NaY, while the the same chiral auxiliary when substituted in the *meta* position (**1g**) gave a maximum of 54% de within RbY (see Table 1). Similarly the L-valine methyl ester amide (**1d**) substitution at the *para* position of mesitylacetophenone gave a maximum of 62% de in RbY while the *meta* substituted counterpart (**1i**) gave maximum of 74% de within NaY. Thus by choosing appropriate MY zeolite and chiral auxiliary, diasteroselectivities in the range of 50–80% can be obtained.

In addition to the asymmetric induction within various cation exchanged zeolites we observed alkali-cation dependent diastereomer switch in all of the *meta*-chiral auxiliary coupled α-mesitylacetophenone

derivatives (**1f–j**) and one of the *para*-chiral auxiliary linked α-mesitylacetophenone derivatives (**1b**) presented in Table 1. For instance, photoreaction of L-valine methyl ester amide of α-mesitylacetophenone (**1i**) gave 74% excess of the B isomer on indan product **2i** within NaY while the KY gave 60% de of the A isomer. The reason we attribute for this switching behavior is the difference in the substrate site to which the alkali metal ions bind on varying the alkali cation within the zeolite framework. This sort of difference in binding pattern between Li^+ and K^+ ions with glycine, valine and arginine has been proposed in the literature [10]. Overall, the influence of chiral auxiliary on enhancement of stereoselectivity on the photo product has been shown to be very effective within MY zeolites when the condition of optimum size and effective binding with the framework cations are met.

Of the several *para* and *meta* chiral auxiliary substituted derivatives synthesized, only four of the substrates (**1a–c**, **1f**) were high melting solids. Photoreaction of these substrates were conducted in crystalline state in order to investigate its effectiveness to conduct asymmetric photoreaction and compare the stereoselectivity thus obtained on the photoproducts with the selectivity obtained within zeolites. Solid-state photoreactions of *para* chiral auxiliary substituted substrates (R)-phenyl ethyl amide (**1a**), (R)-3-methyl-2-butyl amide (**1b**), and S-methoxy propyl amide (**1c**) in the solid state gave 9%, 5% and 22% de on the photo product **2a–c**, respectively, even at low conversions (∼14–17%). However, when the phenyl ethyl amide chiral auxiliary was coupled to the *meta* position of the aryl moiety of mesityl acetophenone (**1f**), the % de obtained on the indanol photo product (**2f**) was 48 for 50% conversion.

In spite of the photochemical reaction occurring in the crystalline state and having a chiral auxiliary attached, which ensures chiral space group, there was no significant asymmetric induction in the photoproduct [11]. The substrates **1b** and **1f** crystallize in chiral space groups C2 and $P2_1$ respectively [12]. Fortunately, the analysis of X-ray crystal structure of **1b** and **1f** revealed the origin of poor stereoselectivity. From Figure 1 it is evident that the carbonyl in the case of **1b** is almost equidistant (3.10 and 3.15 Å) from both the δ-hydrogens and therefore there is nearly an equal preference for abstraction of both the hydrogens.

Unlike substrates **1a–c**, compound **1f** gave better diastereoselectivity (48% for 50% conversion). The single crystals obtained for **1f** were very thin and therefore the crystal structure obtained had an R factor value of 11%. The crystal structure had four independent molecules in the unit cell and in each molecule one of the two δ-hydrogens is closer to the carbonyl chromophore. Among them, three of the molecules have the carbonyl groups tilted toward left side δ-hydrogen and these

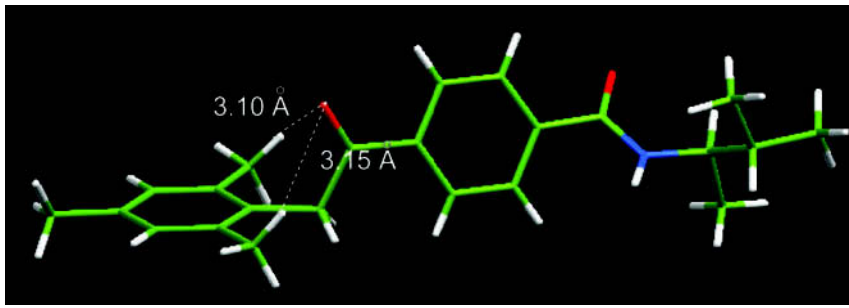

FIGURE 1 X-ray crystal structure of substrate **1b**.

molecules would prefer to abstract the closer hydrogen on the left side and in one of the molecule the carbonyl is tilted towards right side hydrogen (Fig. 2). Theoretically one would expect only a maximum of 50% de to arise on **2f** from these four molecules during photoexcitation of **1f**. Therefore obtaining 48% de for 50% conversion on **2f** is justified.

On the contrary, photoreaction of these four substrates **1a–c**, **1f** within zeolites gave much higher diastereoselectivity compared to the solid-state photoreaction. The % de obtained on these substrates are 60% on **2a** within NaY, 28% on **2b** within NaY, 35% on **2c** in LiY and 45% on **2f** within KY. Even though these diastereoselectivites are moderate, these values are much higher compared to what is obtained in solution media (<7%) and in the solid-state (<22%), except for **2f** which gave up to 32% for 96% conversion in the solid state. One important point to be noted is that the stereoselectivites obtained within zeolites are independent of conversion unlike the solid-state photoreaction which generally undergoes loss of stereochemical control at higher conversions [13]. The other derivatives **1d**, **1e** and **1g–j** were obtained as liquids or low melting solids and therefore were unfit for investigation in the solid-state. On the contrary, these derivatives gave moderate to high de's within zeolite. The notable examples are 62% de on **2d** within RbY, 74% de on **2i** and 57% de on **2j** within NaY.

CONCLUSIONS

Studies presented in this report on diastereoselective photoreaction of α-mesitylacetophenone derivatives establish faujasite zeolite as a reliable host for low to moderate and high diastereoselectivity *via* the chiral auxiliary approach. Though the stereoselectivity obtained with these examples within zeolites are not near quantitative, still it

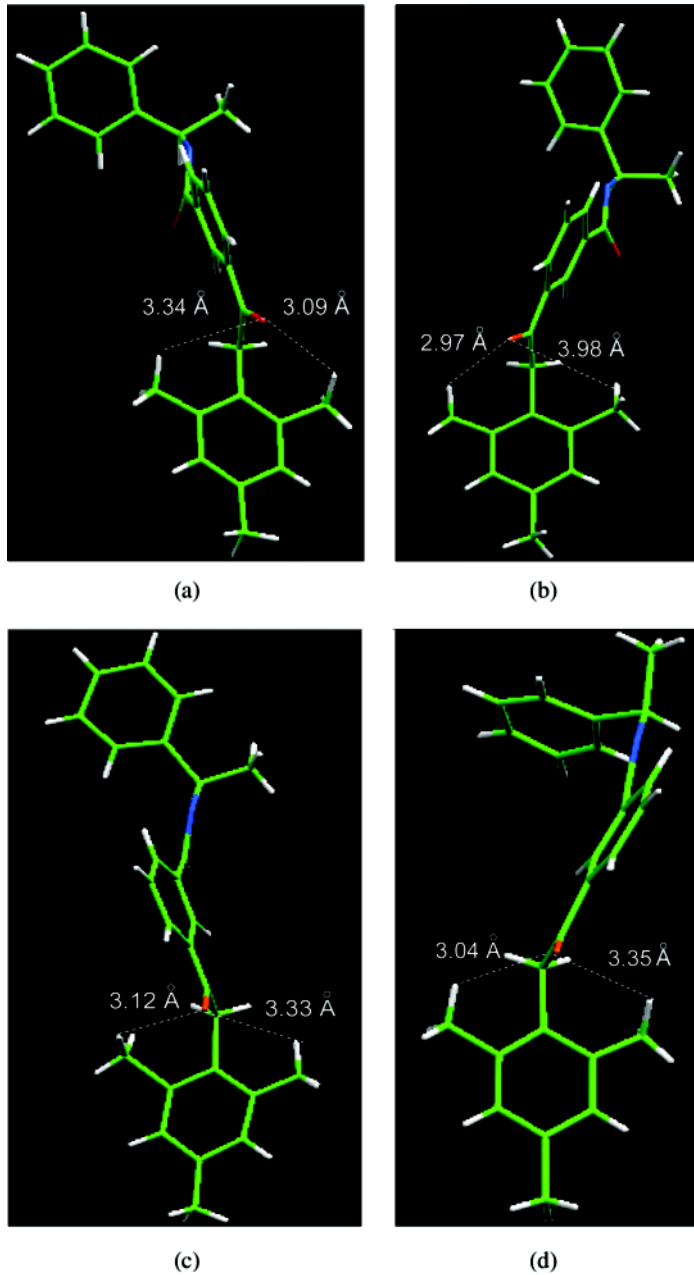

FIGURE 2 X-ray crystal structure of substrate **1f** showing four independent molecules in the asymmetric unit. The structures are shown separately for clarity sake.

allows us to establish the effectiveness of these hosts to conduct asymmetric photoreactions and achieve modest selectivity. There can be little doubt that the chiral influence does get enhanced within zeolites compared to that of isotropic solution. Surprisingly the covalent chiral auxiliary approach failed to preorganize the reactant molecules towards a single diastereomer in the crystalline state in case of the examples of α-mesityacetophenone systems presented. This suggests that the covalent chiral auxiliary approach in the crystalline state can carry inherent problems like crystal melting, occurrence of reaction at defect sites and the cases which involve conformational isomers will give rise to little or no diastereoselectivity in the photoproducts [14]. At such an instance, asymmetric photoreactions conducted within zeolites can become much superior compared to the generally successful crystalline state.

EXPERIMENTAL SECTION

Solution State Photoreaction

Reaction solutions (with < 4 mg ketone) were purged by bubbling nitrogen through the solution for atleast 15 minutes prior to irradiation. During the irradiations the reaction vessel was sealed using septum. Photoproducts were monitored using GC, GC-MS and TLC. The % conversion was kept within 50–60 % to avoid the formation of secondary products.

Photolyses of Ketones within Zeolites

Chiral Auxiliary Approach

The substrate (2 mg) were dissolved in 0.5 ml of dichloromethane and were diluted with 6 mL of hexane. The MY zeolite ($M = Li^+$, Na^+, K^+, Rb^+, Cs^+; 300 mg) activated at 500°C was added to the above solution and stirred for 7–8 h. As the supernatant had trace amount of the unloaded substrate, the sample was filtered and the zeolite was taken into a drying tube and sealed. Then the sample was pre dried in vacuum line was 7–8 hr and the sample was heated at 65°C for 6–7 hr. Later the the drying tube was taken into the dry box and the sample was transferred into a test tube and 6 mL of dry hexane was added to it and the test tube was sealed with rubber septa and parafilm. The irradiation and the analysis part are similar to that as explained in chiral inductor approach. The diastereomeric excesses were analyzed using HPLC (chiralcel-OD, OJ, OC and chiralpak-AD, ADRH).

Solid State Photoreaction and Analysis Procedure

Crystals **1a–c**, **1f** (~5 mg), either as ground single crystals or in polycrystalline form (powder) were sandwiched between two pyrex plates and spread to cover a surface area of 2–3 cm^2. The plates were sealed with parafilm on all the sides before the irradiation process. After the irradiation the solid was dissolved in 2 mL of $CDCl_3$ and analyzed using ^1H NMR. The melting points of the substrates were determined using Mel-Temp apparatus and are uncorrected. Irradiations were performed using 450 W medium-pressure mercury arc lamp in a water-cooled immersion well.

Synthesis of *ortho* and *meta* acids were made following the procedure reported in the literature [7b].

Synthesis of para and meta chiral auxiliary substituted α-mesitylacetopheone derivatives (**1a–1j**): 100 mg of the corresponding acidprecursor was taken in a round bottom flask and to the acid was dissolved in 20 mL of methylene chloride. To this solution 1.2 equivalents of EDC was added and the solution was allowed to stir for 5 min. Later to this solution the corresponding chiral amine or amino acid methyl ester HCl (1.1 equ.) was added the reaction mixture was allowed to stir for 30 mins. The crude reaction mixture was purified using column chromatography (EtOAc:Hexane = 2:8) to yield **1a–j** as white solid.

Characterization of Starting Materials

Compound 1a

^1H NMR (400 MHz, $CDCl_3$): δ 1.62 (d, 3H, J = 7.2 Hz), 2.15 (s, 6H), 2.26 (s, 3H), 4.31 (s, 2H), 5.32–5.36 (m, 1H), 6.34 (d, 1H), 6.88 (s, 2H), 7.28–7.40 (m, 5H), 7.86 (m, 2H, J = 8.4 Hz), 8.08 (d, 2H, J = 8.4 Hz).

GC-MS (EI): 385 (M^+, 29), 253 (8), 252 (100), 133 (88), 120 (15), 105 (48), 104 (27), 103 (21), 78 (19), 58 (15).

Compound 1b

^1H NMR (400 MHz, $CDCl_3$): δ 0.97 (m, 6H), 1.19 (d, 3H, J = 6.4 Hz), 1.82 (m, 1H), 2.17 (s, 6H), 2.27 (s, 3H), 4.09 (m, 1H), 4.32 (s, 2H), 5.94 (d, 1H), 6.89 (s, 2H), 7.85 (m, 2H, J = 8.0 Hz), 8.10 (d, 2H, J = 8.0 Hz).

^{13}C NMR ($CDCl_3$, 100 MHz, δ ppm): 17.9, 18.8, 18.9, 20.5, 21.2, 30.0, 33.4, 39.9, 51, 127.4, 128.5, 129.1, 136.8, 137.0, 139.5, 165.4, 197.5.

Compound 1c

^1H NMR (400 MHz, $CDCl_3$): 1.28 (d, 3H, J = 6.8 Hz), 2.14 (s, 6H), 2.25 (s, 3H), 3.37 (s, 3H), 3.40–3.51 (m, 2H), 4.30 (s, 2H), 4.35–4.39 (m, 1H), 6.44 (d, 1H), 6.87 (s, 2H), 7.85 (m, 2H, J = 8.4 Hz), 8.07 (d, 2H, J = 8.4 Hz).

^{13}C NMR ($CDCl_3$, 100 MHz, δ ppm): 17.9, 20.5, 21.2, 30.0, 40.0, 45.9, 59.5, 75.6, 127.6, 128.5, 129.2, 136.8, 137.0, 139, 139.4, 160.0, 197.2.

Compound 1d

^{1}H NMR (400 MHz, $CDCl_3$): 0.97–1.02 (dd, 6H, J = 9.6 Hz), 2.16 (s, 6H), 2.26 (s, 3H), 2.28–2.32 (m, 1H), 3.78 (s, 3H), 4.32 (s, 2H), 4.77–4.80 (q, 1H, J = 8.8 Hz), 6.69 (d, 1H), 6.88 (s, 2H), 7.90 (m, 2H, J = 8.8 Hz), 8.11 (d, 2H, J = 8.8 Hz).

^{13}C NMR ($CDCl_3$, 100 MHz, δ ppm): 17.9, 18.2, 20.5, 21.2, 31.8, 40.0, 52.6, 59.0, 127.6, 128.6, 129.1, 129.2, 136.8, 137.0, 138.2, 139.6, 166.2, 172.4, 197.5.

Compound 1e

^{1}H NMR (400 MHz, $CDCl_3$): 0.97–1.02 (dd, 6H, J = 8.0 Hz), 1.63–1.78 (m, 2H), 2.16 (s, 6H), 2.26 (s, 3H), 3.77 (s, 3H), 4.32 (s, 2H), 4.83–4.89 (m, 1H), 6.63 (d, 1H), 6.88 (s, 2H), 7.89 (m, 2H, J = 8.8 Hz), 8.09 (d, 2H, J = 8.8 Hz).

^{13}C NMR ($CDCl_3$, 100 MHz, δ ppm): 20.5, 21.2, 22.3, 23.1, 27.0, 39.9, 42.1, 51.4, 52.7, 127.7, 128.5, 129.1, 129.2, 136.8, 137.0, 138.0, 139.6, 166.2, 173.8, 197.0.

Compound 1f

^{1}H NMR (400 MHz, $CDCl_3$): δ 1.61 (d, 3H, J = 7.2 Hz), 2.15 (s, 6H), 2.26 (s, 3H), 4.34 (s, 2H), 5.318–5.36 (m, 1H), 6.45 (d, 1H), 6.87 (s, 2H), 7.27–7.38 (m, 5H), 7.56 (t, 1H, J = 15.6 Hz), 8.00 (m, 1H), 8.17 (m, 1H), 8.41 (t, 1H, J = 3.6 Hz).

^{13}C NMR ($CDCl_3$, 100 MHz, δ ppm): 20.54, 21.18, 21.89, 39.91, 49.7, 126.50, 126.57, 127.86, 129.05, 129.11, 129.34, 131.15, 131.76, 135.24, 136.76, 137.0, 137.43, 143.0, 165.77, 196.97.

Compound 1g

^{1}H NMR (400 MHz, $CDCl_3$): δ 0.97 (dd, 6H), 1.19 (d, 3H, J = 6.4 Hz), 1.80 (m, 1H), 2.17 (s, 6H), 2.27 (s, 3H), 4.0–4.12 (m, 1H), 4.35 (s, 2H), 6.02 (d, 1H), 6.89 (s, 2H), 7.56 (t, 1H, J = 15.6 Hz), 8.00 (m, 1H), 8.18 (m, 1H), 8.40 (t, 1H, J = 3.6 Hz).

Compound 1h

^{1}H NMR (400 MHz, $CDCl_3$): 1.29 (d, 3H, J = 6.8 Hz), 2.16 (s, 6H), 2.26 (s, 3H), 3.37 (s, 3H), 3.40–3.51 (m, 2H), 4.30 (s, 2H), 4.35–4.40 (m, 1H), 6.51 (d, 1H), 6.88 (s, 2H), 7.57 (t, 1H, J = 15.6 Hz), 8.00 (m, 1H), 8.17 (m, 1H), 8.43 (t, 1H, J = 3.6 Hz).

Compound 1i

^{1}H NMR (400 MHz, $CDCl_3$): 0.97–1.02 (dd, 6H, J = 9.6 Hz), 2.16 (s, 6H), 2.26 (s, 3H), 2.28–2.32 (m, 1H), 3.78 (s, 3H), 4.36 (s, 2H),

4.77–4.80 (q, 1H, J = 8.8 Hz), 6.74 (d, 1H), 6.88 (s, 2H), 7.60 (t, 1H, J = 15.6 Hz), 8.02 (m, 1H), 8.20 (m, 1H), 8.49 (t, 1H, J = 3.6 Hz).

^{13}C NMR ($CDCl_3$, 100 MHz, δ ppm): 18.2, 19.26, 20.54, 21.18, 31.8, 39.7, 39.8, 52.62, 57.86, 126.99, 129.01, 129.11, 129.15, 129.38, 131.38, 131.62, 134.85, 136.74, 137.01, 137.59, 166.72, 172.76, 196.85.

Compound 1j

^{1}H NMR (400 MHz, $CDCl_3$): 0.91–0.95 (dd, 6H, J = 6.8 Hz), 1.60–1.73 (m, 2H), 2.10 (s, 6H), 2.22 (s, 3H), 3.71 (s, 3H), 4.30 (s, 2H), 4.78–4.85 (m, 1H), 6.59 (d, 1H), 6.84 (s, 2H), 7.60 (t, 1H, J = 15.2 Hz), Hz), 7.96 (m, 1H), 8.16 (m, 1H), 8.42 (t, 1H, J = 3.6 Hz).

^{13}C NMR ($CDCl_3$, 100 MHz, δ ppm): 20.52, 20.57, 21.23, 22.2, 23.08, 25.2, 39.8, 41.9, 51.55, 52.8, 126.8, 126.93, 129.08, 129.15, 129.34, 134.61, 136.8, 137.0, 137.6, 166.46, 173.79, 196.85.

Characterization of Photoproducts

Photoproduct 2a

^{1}H NMR (400 MHz, $CDCl_3$): δ 1.60 (d, 3H, J = 6.8 Hz), 2.22 (s, 3H), 2.30 (s, 3H), 3.17–3.24 (AB quart, 2H, J = 16 Hz), 3.32–3.49 (AB quart, 2H, J = 16 Hz), 4.01–4.13 (m, 1H), 5.28–5.36 (m, 1H), 6.28 (d, 1H), 6.87 (s, 1H), 6.92 (s, 1H), 7.25–7.40 (m, 5H), 7.62 (m, 2H, J = 8.8 Hz), 7.75 (d, 2H, J = 8.8 Hz).

Photoproduct 2b

^{1}H NMR (400 MHz, $CDCl_3$): δ 0.93–0.96 (dd, 6H, J = 6.8 Hz), 1.16 (d, 3H, J = 6.4 Hz), 2.22 (s, 3H), 2.30 (s, 3H), 3.17–3.24 (AB quart, 2H, J = 16.4 Hz), 3.32–3.50 (AB quart, 2H, J = 16.4 Hz), 4.04–4.10 (m, 1H), 5.88 (d, 1H), 6.87 (s, 1H), 6.92 (s, 1H), 7.63 (m, 2H, J = 8.4 Hz), 7.75 (d, 2H, J = 8.4 Hz).

Photoproduct 2c

^{1}H NMR (400 MHz, $CDCl_3$): δ 1.28 (d, 3H, J = 6.8 Hz), 2.22 (s, 3H), 2.30 (s, 3H), 3.17–3.24 (AB quart, 2H, J = 16.0 Hz), 3.32–3.50 (m, 4H), 3.37 (s, 3H), 4.04–4.10 (m, 1H), 4.34–4.4 (m, 1H), 6.35 (d, 1H), 6.87 (s, 1H), 6.92 (s, 1H), 7.62 (m, 2H, J = 8.4 Hz), 7.75 (d, 2H, J = 8.4 Hz).

Photoproduct 2d

^{1}H NMR (400 MHz, $CDCl_3$): δ 0.96–1.0 (dd, 6H, J = 10.0 Hz), 2.22 (s, 3H), 2.30 (s, 3H), 3.17–3.25 (AB quart, 2H, J = 16.4 Hz), 3.33–3.50 (AB quart, 2H, J = 16 Hz), 3.76 (s, 3H), 4.76–4.79 (q, 1H, J = 8.0 Hz),

6.60 (d, 1H), 6.87 (s, 1H), 6.92 (s, 1H), 7.64 (m, 2H, J = 8.0 Hz), 7.75 (d, 2H, J = 8.0 Hz).

Photoproduct 2e

^{1}H NMR (400 MHz, $CDCl_3$): δ 0.96–0.99 (dd, 6H, J = 8.4 Hz), 1.63–1.78 (m, 2H), 2.22 (s, 3H), 2.31 (s, 3H), 3.17–3.25 (AB quart, 2H, J = 16.0 Hz), 3.33–3.50 (AB quart, 2H, J = 16.4 Hz), 3.76 (s, 3H), 4.86–4.79 (m, 1H), 6.49 (d, 1H), 6.88 (s, 1H), 6.92 (s, 1H), 7.65 (m, 2H, J = 8.4 Hz), 7.79 (d, 2H, J = 8.4 Hz).

Photoproduct 2f

^{1}H NMR (400 MHz, $CDCl_3$): δ 1.60 (d, 3H, J = 6.8 Hz), 2.2 (s, 3H), 2.3 (s, 3H), 3.17–3.24 (AB quart, 2H, J = 16.0 Hz), 3.34–3.51 (AB quart, 2H, J = 16.0 Hz), 5.318–5.36 (m, 1H), 6.33 (d, 1H), 6.86 (s, 1H), 6.92 (m, 1H), 7.26–7.42 (m, 6H), 7.67 (m, 1H), 8.00 (m, 1H).

Photoproduct 2g

^{1}H NMR (400 MHz, $CDCl_3$): δ 0.97 (dd, 6H), 1.19 (d, 3H, J = 6.4 Hz), 1.80 (m, 1H), 2.2 (s, 3H), 2.31 (s, 3H), 3.18–3.26 (AB quart, 2H, J = 16.0 Hz), 3.36–3.53 (AB quart, 2H, J = 16.0 Hz), 4.0–4.12 (m, 1H), 5.9 (d, 1H), 6.87 (s, 1H), 6.93 (m, 1H), 7.41 (t, 1H, J = 15.6 Hz), 7.63–7.67 (m, 2H), 7.98 (t, 1H, J = 3.6 Hz).

Photoproduct 2h

^{1}H NMR (400 MHz, $CDCl_3$): δ 1.29 (d, 3H, J = 6.8 Hz), 2.2 (s, 3H), 2.31 (s, 3H), 3.18–3.26 (AB quart, 2H, J = 16.0 Hz), 3.36–3.53 (m, 4H), 3.7 (s, 3H), 4.35 (m, 1H), 6.36 (d, 1H), 6.87 (s, 1H), 6.92 (m, 1H), 7.41 (t, 1H), 7.63–7.67 (m, 2H), 8.0 (t, 1H).

Photoproduct 2i

^{1}H NMR (400 MHz, $CDCl_3$): δ 0.97–1.01 (dd, 6H, J = 10.0 Hz), 1.19 (d, 3H, J = 6.4 Hz), 1.80 (m, 1H), 2.2 (s, 3H), 2.31 (s, 3H), 2.28–2.32 (m, 1H), 3.19–3.26 (AB quart, 2H, J = 16.0 Hz), 3.36–3.53 (AB quart, 2H, J = 16.0 Hz), 3.76 (s, 3H), 4.76–4.8 (q, 1H, J = 8.8 Hz), 6.63 (d, 1H), 6.87 (s, 1H), 6.93 (m, 1H), 7.43 (t, 1H, J = 8.0 Hz), 7.68–7.73 (m, 2H), 8.05 (t, 1H).

Photoproduct 2j

^{1}H NMR (400 MHz, $CDCl_3$): 0.91–0.95 (dd, 6H, J = 6.8 Hz), 1.60–1.73 (m, 2H), 2.2 (s, 3H), 2.31 (s, 3H), 3.19–3.26 (AB quart, 2H, J = 16.0 Hz), 3.36–3.53 (AB quart, 2H, J = 16.0 Hz), 3.71 (s, 3H), 4.78–4.85 (m, 1H), 6.59 (d, 1H), 6.87 (s, 1H), 6.93 (m, 1H), 7.43 (t, 1H, J = 8.0 Hz), 7.68–7.73 (m, 2H), 8.05 (t, 1H).

REFERENCES

[1] Inoue, Y. & Ramamurthy, V. (Eds.), (2004). *Chiral Photochemistry*, Marcell Dekker: New York, Vol. 11, 129.

[2] a) Rau, H. (2004). In: *Chiral Photochemistry*, Inoue, Y. & Ramamurthy, V. (Eds.), Marcel Dekker: New York; b) Hammond, G. S. & Cole, R. S. (1965). *J. Am. Chem. Soc.*, *87*, 3256–3257; c) Grosch, B. & Bach, T. (2004). In: *Chiral Photochemistry*, Inoue, Y. & Ramamurthy, V. (Eds.), Marcel Dekker: New York, Vol. 11, 315; d) Elgavi, A., Green, S. B., & Schmidt, G. M. J. (1973). *J. Am. Chem. Soc.*, *95*, 2058–2059; e) Scheffer, J. R. (2001). *Can. J. Chem.*, *79*, 349–357; f) Toda, F. (1995). *Acc. Chem. Res.*, *28*, 480–486.

[3] a) Garcia-Garibay, M., Scheffer, J. R., Trotter, J., & Wireko, F. (1989). *J. Am. Chem. Soc.*, *111*, 4985–4986; b) Ohasi, Y., Sakai, Y., Sekine, A., Arai, Y., Ohgo, Y., Kamiya, N., & Iwasaki, H. (1995). *Bull. Chem. Soc. Jpn.*, *68*, 2517; c) Leibovitch, M., Olovsson, G., Scheffer, J. R., & Trotter, J. (1997). *Pure & Appl. Chem.*, *69*, 815–823; d) Toda, F. (1995). *Acc. Chem. Res.*, *28*, 480–486.

[4] Natarajan, A., Mague, J. T., & Ramamurthy, V. (2005). *J. Am. Chem. Soc.*, *127*, 3568; Natarajan, A., Mague, J. T., & Ramamurthy, V. (2005). *Crystal Growth and Design*, *5*, 2348.

[5] Ramamurthy, V., Natarajan, A., Kaanumalle, L. S., Karthikeyan, S., Sivaguru, J., Shailaja, J., & Joy, A. (2004). Chiral photochemistry within zeolites. In: *Chiral Photochemistry*, Inoue, Y. & Ramamurthy, V. (Eds.), Marcell Dekker: New York, 563–633.

[6] Sivaguru, J., Natarajan, A., Kaanumalle, L. S., Shailaja, J., Uppili, S., Joy, A., & Ramamurthy, V. (2003). *Acc. Chem. Res.*, *36*, 509–521.

[7] a) Wagner, P. J., Meador, M. A., Zhou, B., & Park, B.-S. (1991). *J. Am. Chem. Soc.*, *113*, 9630; b) Cheung, E., Rademacher, K., Scheffer, J. R., & Trotter, J. (2000). *Tetrahedron*, *56*, 6739–6751.

[8] Procedure for loading, photoreaction, extraction are presented in the supplementary material.

[9] Kaanumalle, L. S., Sivaguru, J., Arunkumar, N., Karthikeyan, S., & Ramamurthy, V. (2003). *Chem. Commun.*, *1*, 116–117.

[10] Jockusch, R. A., Lemoff, A. S., & Williams, E. R. (2001). *J. Am. Chem. Soc.*, *123*, 12255.

[11] Crystals **3b**, **3d** were mounted in Cryoloops™ with Paratone oil and placed in the cold nitrogen stream of the Kryoflex™ attachment of the Bruker APEX CCD diffractometer (Bruker-AXS-2000). Full spheres of data were collected using 606 scans in ω (0.3° per scan) at $\varphi = 0$, 120 and 240°. The raw data were reduced to F^2 values using the SAINT+ software (Version 7.03, Madison WI). Multiple measurements of equivalent reflections provided the basis for empirical absorption corrections as well as corrections for any crystal deterioration during the data collection (SADABS, Version 2.05, University of Gottingen, Germany). The structures were completed by successive cycles of full-matrix, least-squares refinement followed by the calculation of difference maps. All hydrogen atoms attached to carbon were placed in calculated positions with isotropic displacement parameters 20% larger than those of the attached atoms and allowed to ride. All computations associated with structure solution, refinement and presentation were performed with the SHELXTL (Version 6.10, Madison, WI) package. The cavity plots were obtained using PLATON program (Spek, A. L. 2005; Utrecht University, Netherlands). For crystal structure visualization MERCURY (CSD software)[16] was used; Bruno, I. J., Cole, J. C., Edgington, P. R., Kessler, M. K., Macrae, C. F., McCabe, P., Pearson, J., & Taylor, R. (2001). *Acta Crystallogr.*, *B58*, 815.

[12] **1b**. $C_{23}H_{29}NO_2$, M = 351.47, transperant, colorless plate (0.22 × 0.13 × 0.09), Monoclinic, C2, a = 16.142(6), b = 8.797(3), c = 15.396(6), β = 112.019(6), V = 2026.8(13), Z = 4, 4643 reflections collected, R = 4.0%. **1f**. $C_{26}H_{27}NO_2$, M = 385.49, transparant, colorless needle (0.32 × 0.05 × 0.02), Monoclinic, $P2_1$, a = 9.602(6), b = 18.051(3), c = 26.304(6), β = 93.568(6), V = 4550.3(13), Z = 8, 25334 reflections collected, R = 11.0%. The crystal **1f** was twinned and therefore averaging Friedel opposites can't be done reliably because not all symmetry equivalent reflections have the same amount of overlap (or its absence) between the twin components. Also the quality of the data set was poor due to very small crystal size.

[13] Keating, A. E. & Garcia-Garibay, M. A. (1998). Photochemical solid-to-solid reactions. In: *Molecular and Supramolecular Photochemistry*, Ramamurthy, V. & Schanze, K. S. (Eds.), Marcel Dekker, Inc.: New York, 195–248.

[14] a) Scheffer, J. R. (2004). The Solid-state ionic chiral auxiliary approach to asymmetric induction in photochemical reactions. In: *Chiral Photochemistry*, Ramamurthy, V. (Ed.), Marcell Dekker: New York, 463–483; b) Natarajan, A., Wang, K., Ramamurthy, V., Scheffer, J. R., & Patrick, B. (2002). *Org. Lett.*, *4*, 1443–1446.